

Clinical Data Sets of Human Immunodeficiency Virus Type 1 Reverse Transcriptase-Resistant Mutants Explained by a Mathematical Model

NIKOLAOS I. STILIANAKIS,¹ CHARLES A. B. BOUCHER,² MENNO D. DE JONG,³
REMKO VAN LEEUWEN,³ ROB SCHUURMAN,² AND ROB J. DE BOER^{4*}

*Theoretical Division, Group T-10, Los Alamos National Laboratory, Los Alamos, New Mexico 87545,¹ and
Department of Clinical Microbiology, Utrecht University, 3508 GA Utrecht,² National AIDS Therapy
Evaluation Centre, University of Amsterdam, Academic Medical Centre,³ and Theoretical Biology,
Utrecht University, 3584 CH Utrecht,⁴ The Netherlands*

Received 8 March 1996/Accepted 16 September 1996

Treatment of human immunodeficiency virus type 1 (HIV-1) infection during the clinical latency phase with drugs inhibiting reverse transcriptase (RT) reduces the HIV-1 RNA load and increases the CD4⁺ T-cell count. Typically, however, the virus evolves mutations in the RT gene that circumvent the drugs. We develop a mathematical model for this situation. The model distinguishes quiescent from activated CD4⁺ T cells, incorporates the fact that only activated cells can become productively infected by HIV-1, embodies empirical estimates for the drug resistance and the mutation frequency for each of the HIV-1 drug-resistant mutants, and assumes the antiviral immune response to remain constant over the course of the experiments. We analyze clinical data on the evolution of drug-resistant mutants for the RT inhibitors lamivudine and zidovudine. The results show that the evolutionary sequence of the drug-resistant mutants in both data sets is accounted for by our model, given that lamivudine is more effective than zidovudine. Thus, current empirical estimates of the mutation frequencies and the drug resistances of the mutants suffice for explaining the data. We derive a critical treatment level below which the wild-type HIV-1 RNA load can rebound before the first drug-resistant mutant appears. Our zidovudine data confirm this to be the case. Thus, we demonstrate in the model and the data that the rebound of the HIV-1 RNA load in the case of zidovudine is due to the outgrowth of wild-type virus and the first drug-resistant mutant, whereas that in the case of lamivudine can only be due to the drug-resistant mutants. The evolution of drug resistance proceeds slower in the case of zidovudine because (i) zidovudine is not as effective as lamivudine and (ii) the first zidovudine drug-resistant mutant is competing with the rebounding wild-type virus.

The emergence of human immunodeficiency virus type 1 (HIV-1) isolates resistant to protease- and reverse transcriptase (RT)-inhibiting drugs during treatment is well documented in several clinical studies (3, 21, 22, 34, 36). One observes a fast reduction of the HIV-1 RNA load, which is typically accompanied by an increase of CD4⁺ T-cell counts. After several weeks of treatment, however, the viral RNA load rebounds. The rebound is frequently, i.e., not always (8), associated with the appearance of drug-resistant mutants. Genotypic analysis demonstrates that the resistance to RT is caused by specific amino acid changes at certain codons in the HIV-1 RT gene (21, 22). These point mutations appear in a typical order and in the case of zidovudine become combined, conferring higher resistance (4, 8, 35). Similarly, the protease studies describe mutations in the HIV-1 protease gene (36).

In this report, we first investigate whether the data that we have on the mutation frequencies and drug resistance of the mutants can explain the precise evolutionary order in which the mutants arise. This question is addressed for two independent clinical data sets on treatment with lamivudine (35) and zidovudine (8). Since the model indeed explains the precise evolutionary order, we find good agreement between model and data. Second, data obtained from treatment with zidovudine demonstrate that the HIV-1 RNA load rebounds before the drug-resistant mutants appear (8). We describe that such a

rebound of the HIV-1 RNA load can adequately be explained by the increase of the CD4⁺ T-cell population during treatment.

Our model extends previous mathematical models for the dynamics of the HIV-1 infection of the CD4⁺ target cells (11, 32) and for evolution of drug-resistant mutants (14, 28) because we (i) use recently derived parameters indicating that HIV-1 infection is very dynamic process (17, 36) and (ii) incorporate recent detailed parameter estimates for the drug resistance and the mutation frequency of the mutants.

MATERIALS AND METHODS

Model. HIV-1-infected individuals typically have a long clinical latency phase in which (i) HIV-1 is present abundantly in lymphoid organs (9, 31), (ii) the CD4⁺ population is lower than normal (14), and (iii) HIV-1 and HIV-infected CD4⁺ cells are turning over rapidly (17, 36). Our model describes a particular time point somewhere in the clinical latency phase. This time point is an equilibrium between HIV-1 infection and T-cell renewal. We study the effects of treatment with drugs inhibiting the HIV-1 infection process. The essential assumption in our model is that the immune response to the virus remains invariant over the time course of the clinical experiments. By this assumption, HIV-1 is (transiently) limited by availability of target CD4⁺ T cells (5, 6). The typical response of HIV-1 to drug treatment is the evolution of drug-resistant mutants. The drug resistance of these mutants is known and is incorporated in the model. In the model, we distinguish quiescent CD4⁺ T cells Q , target cells or activated CD4⁺ T cells T , and virus particles V_j and productively infected CD4⁺ T cells I_j for virus strain j (Fig. 1).

In adults, the CD4⁺ T-cell compartment is largely maintained by self-renewal (25). Hence we allow the quiescent CD4⁺ T cells to become activated by low-level activation at a rate α , they die at a rate δ_Q , and they appear by the proliferation of activated T cells at a maximum rate r ; i.e., we write

* Corresponding author. Mailing address: Theoretical Biology, Utrecht University, Padualaan 8, 3584 CH Utrecht, The Netherlands.

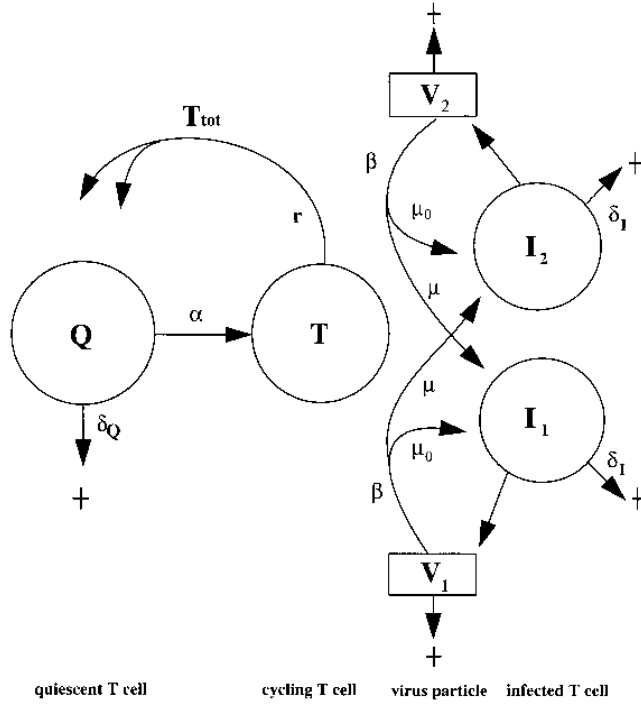


FIG. 1. A scheme of the model. Resting T cells Q become activated at a rate α and die at a rate δ_Q . Activated cells T return to the quiescent state after division into two daughter cells at a rate r . Viral particles V infect activated cells at a rate β , thus generating productively infected cells I . V_1 and I_1 denote one particular strain of virus; V_2 with I_2 denote another strain. The μ parameters represent mutation: at a rate μ , a viral strain copies itself correctly; at a rate μ , however, RT errors create novel strains. Productively infected T cells I are cleared at a rate δ_I .

$$\frac{dQ}{dt} = \frac{2rT}{1 + T_{\text{tot}}/T_{\text{max}}} - (\alpha + \delta_Q)Q \quad (1)$$

where the $2/(1+T_{\text{tot}}/T_{\text{max}})$ term defines a density-dependent regulation of the proliferation rate. When $T_{\text{tot}} = T_{\text{max}}$, proliferation stops. The activated CD4^+ T cells T appear by activation of quiescent cells, they revert to the quiescent stage at a rate r , and they are infected by all virus strains at a rate β weighted by the total RT fitness f_j of the strain; i.e., we write

$$\frac{dT}{dt} = \alpha Q - rT - \beta T \sum_j f_j V_j \quad (2)$$

where the sum term says that CD4^+ T cells are infected by all virus strains at a rate weighted by the total fitness of the strain.

The productively infected CD4^+ T cells appear by the infection of target cells by virus. Because infection may involve mutations, i.e., RT errors, we implement a mutation matrix M incorporating the estimated mutation frequencies. Matrix element M_{jl} is the mutation frequency by which strain j appears from strain l . Thus, the diagonal elements M_{jj} give the frequency at which strain j correctly transcribes itself. Hence we write

$$\frac{dI_j}{dt} = \beta T \sum_l M_{jl} f_l V_l - \delta_I I_j \quad (3)$$

where δ_I is the turnover rate of productively infected cells. Thus, the total number of CD4^+ T cells in our model is defined by $T_{\text{tot}} = Q + T + \sum_j I_j$.

Assuming that the virus density is proportional to the density of infected CD4^+ T cells, and appropriate scaling, allows us to write $V_j = I_j$. Hence we may arbitrarily define the total HIV-1 RNA load as $\text{RNA} = 10^4 \sum V_j$ copies per ml, which gives realistic viral RNA loads (see below). The estimated half-life of quiescent CD4^+ T cells is about 1,000 days (29); i.e., we set $\delta_Q = 10^{-3}$ per day. Activated cells revert to the quiescent stage by a single cell division at a rate of one per day (i.e., $r = 1$ per day). Because in normal individuals about 2% of the T cells are activated, we set $\alpha = 0.02$ per day as the activation rate of quiescent cells. Setting $T_{\text{max}} = 1,100$ cells per μl , we obtain an equilibrium of about 1,000 CD4^+ T cells per μl (26). The turnover of productively infected cells, which can

be due to an effective cellular immune response or to viral cytopathicity, is estimated to be $\delta_I = 0.5$ per day (17, 33, 36). The *in vivo* infection rate is not known. Setting $\beta = 0.05$, we obtain reasonable CD4^+ T-cell counts (see below).

Fitness. Each of the virus strains has a total RT fitness f_j which combines the fitness in the absence of the drug with the drug resistance in its presence. Previous estimates for the fitness of drug-resistant mutants in the absence of RT were just a few percent less than that of the wild-type virus (5, 15). Recent experiments, however, suggest that these fitness differences may be considerable, i.e., more than 10% (1, 16, 30a). Here we scale the fitness of the wild-type virus to 1, i.e., we set $e_{\text{wt}} = 1$, and conservatively choose as a default value for the fitness of all mutant strains $e_j = 0.99$. For the fitness in the presence of the drug f_j , we use the conventional notion of the IC_{50} , which is the drug concentration at which the effect of the drug is half-maximal. Thus, we employ the classical saturation function for the IC_{50} (18), describing the drug resistance as

$$f_j = \frac{e_j}{1 + D/R_j} \quad (4)$$

where D is the effective drug concentration and R_j is the IC_{50} of strain j . We consider only mutants with a resistance higher than that of the wild-type virus. Hence, we again scale $R_{\text{wt}} = 1$ and require for all mutants j that $R_j > 1$. In the absence of the drug, i.e., when $D = 0$, the fitness is defined by the RT fitness e_j . In the presence of the drug, the total fitness becomes half-maximal at an effective drug concentration of $D = R_j$.

Mutation frequencies. In our data sets, we consider mutations in the RT gene providing resistance to the RT inhibitors. The first measure to include in the mutation matrix is the number of nucleotide changes that are involved in going from strain l to strain j . Recent work (27) showed that the basic error rate of RT is on the order of 3×10^{-5} mutations per nucleotide and that about two-thirds of the mutations are base pair substitutions. In the context of the RT gene, however, different nucleotide changes are not equally probable. It is well established that the G→A mutation is preferred over all others. Indeed, about half of the 2×10^{-5} base pair substitutions per nucleotide are G→A point mutations (27). Our G→A mutation frequency is therefore set to $\mu_1 = 10^{-5}$ per nucleotide. Five other mutations are involved in our study: A→G, C→A, A→C, T→A, and A→T. The last four would be least probable because they involve transversions. Following Keulen et al. (20), we therefore classify the mutation rates into three classes, $\mu_1 > \mu_2 > \mu_3$, setting $P(\text{G} \rightarrow \text{A}) = \mu_1$, $P(\text{A} \rightarrow \text{G}) = \mu_2$, and $P(\text{C} \rightarrow \text{A}) = P(\text{A} \rightarrow \text{C}) = P(\text{T} \rightarrow \text{A}) = P(\text{A} \rightarrow \text{T}) = \mu_3$. Due to a lack of good data for the low-frequency mutations, we arbitrarily set the last two rates to $\mu_2 = \mu_1/2$ and $\mu_3 = \mu_1/10$. The frequency M_{jj} that a virus correctly copies itself can be approximated by considering that RT is 1,680 bases long and that the basic error rate is on the order of 3×10^{-5} (27); i.e., we set $M_{jj} = \mu_0 = (1 - 3 \times 10^{-5})^{1680} \approx 0.95$. We model mutation as a continuous process, which implies that all mutants are present at low frequency before the onset of treatment (30). We ignore mutations involving more than two nucleotide changes; i.e., the minimum mutation frequency that we consider is μ_3^2 .

Disease progression. During the clinical latency stage, disease progression is characterized by slowly decreasing CD4 counts and slowly increasing HIV-1 RNA levels. The patients in our data have different CD4 counts and are thus assumed to be in different stages of disease progression. Because we pick just one time point in the clinical latency phase, we here refrain from modeling disease progression. However, we have to be able to study different time points, i.e., patients with different CD4 counts. Since disease progression is associated with hyperactivation of the immune system (12), we model progression by setting different values for α , the T-cell activation rate. Increasing α indeed decreases the CD4 count and increases the viral load (7). The data supporting this (17) are discussed below.

RESULTS

Our detailed data on the evolution of HIV-1 drug-resistant mutants consider mutations in RT selected during treatment with either zidovudine (8) or lamivudine (35). These two drugs differ in efficacy (10). With respect to the nadir, serum levels of HIV-1 RNA drop 1 to 2 logs in about a week with lamivudine treatment (35), whereas administration of zidovudine leads to a drop of fourfold in 2 to 4 weeks (8, 24). The two drugs also differ in the time scale of the rebound in the HIV-1 RNA load, which is 2 to 3 weeks for lamivudine (35) and 2 months for zidovudine (8). We show that these differences in amplitude and time scale can adequately be explained by a difference in effective drug concentration D . Recent studies estimated the dynamics of HIV-1 RNA and CD4^+ T-cell turnover in analyser using potent protease or RT inhibitors (17, 36). The effectiveness of these drugs is comparable to that of lamivudine. We therefore model all of these data sets by considering a low effective drug concentration in the case of zidovudine (where

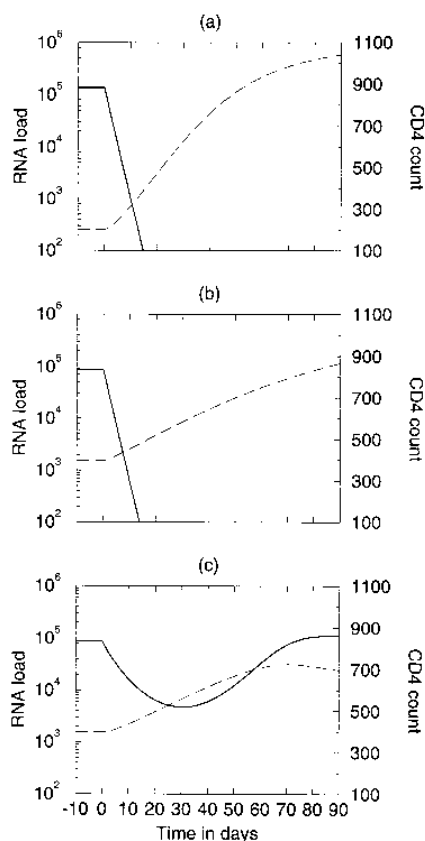


FIG. 2. The parameters of the model are confirmed by comparing them to recent data (17, 36). Parameters: $r = 1$, $T_{\max} = 1,100$, $\beta = 0.05$, $\delta_D = 0.01$, $\delta_T = 0.5$, $e_{\text{wt}} = 1$, $R_{\text{wt}} = 1$, and $\mu_0 = 0.95$. In this figure, mutations into drug-resistant mutants are switched off, i.e., $\mu_1 = \mu_2 = \mu_3 = 0$. (a) $\alpha = 0.1$ and $D = 100$; (b) $\alpha = 0.04$ and $D = 100$; (c) $\alpha = 0.04$ and $D = 1$.

$D \leq 1$ are our typical values) and a high effective drug concentration in all other cases (i.e., $D = 100$ is our typical value). We first study how our model fits the recently estimated dynamic parameters (17, 36).

Dynamics in the absence of mutation. The empirical data are obtained from the rates at which CD4 counts recover following anti-HIV-1 treatment (17, 36). We now perform the same treatment in our model and ignore mutation by setting $\mu_1 = \mu_2 = \mu_3 = 0$ (Fig. 2). In the protease data, the average CD4 count is on the order of 200 CD4⁺ cells per μl (17, 36). In Fig. 2a, we choose $\alpha = 0.1$ so that the equilibrium at day 0 has $T_{\text{tot}} \approx 200$. The average CD4 count in the zidovudine data is about 400 CD4⁺ cells (8). Thus, in Fig. 2b and c, we set $\alpha = 0.04$ in order to have $T_{\text{tot}} \approx 400$. In Fig. 2a and b, we depict a very effective drug (like ritonavir or lamivudine) by setting $D = 100$ at day 0; in Fig. 2c, we depict a less effective drug (like zidovudine) by setting $D = 1$ at day 0.

The model behavior corresponds closely with the data. The rate at which the viral RNA level decreases strongly depends on the effective drug concentration D . In Fig. 2a and b, where $D = 100$, the viral RNA level decreases with exactly the same slope as is reported in the recent empirical data (17, 36), i.e., with a slope δ_T (see Appendix). For the potent drugs, this slope is rather independent of the CD4 count: the slopes are very similar in Fig. 2a and b. This is also the case in the data of Ho *et al.* (17). The slopes with which the CD4 counts recover depend on the initial CD4 count, as they do in the published

data (17). In Fig. 2a and b, the exponential slopes, i.e., $\{ \ln[T_{\text{tot}}(10)]/T_{\text{tot}}(0) \}/10$, are 0.04 and 0.01, respectively. For CD4 counts of 200 and 400, respectively, these two values match the data (17).

The picture becomes much more complicated when the drug is less effective, as is the case for the zidovudine data. For $D = 1$, we show in Fig. 2c that the slope with which the viral RNA level declines is less steep. In the appendix, we show that this slope is determined by a combination of factors: the total fitness of the wild-type virus, the initial CD4 count, and the CD4 recovery rate. Because the viral RNA level decreases only slowly, the rate at which the CD4 level recovers is also slow. We conclude that the time scale at which the viral RNA level drops and the CD4 count recovers is determined by the effective drug concentration D .

In Fig. 2c, we observe that after a month of treatment, the viral RNA level rebounds. If we were to run this simulation longer, the system would approach a new equilibrium in which the HIV-1 RNA load is similar to that of day 0, while CD4⁺ T-cell counts have approximately doubled. Thus, halving the fitness, by setting $D = 1$ (equation 4), approximately doubles the CD4 count. Since there are no drug-resistant mutants in this simulation, the viral rebound is entirely due to the recovery of the CD4⁺ cells (which increases the virus growth rate). Exactly the same phenomenon is observed in our data: after a month of zidovudine treatment, virus RNA levels rebound (8). In the data, this happens before the first drug-resistant mutants appear. The rebound, being due to the recovery of the CD4⁺ cells, is therefore nothing more than a classical predator-prey oscillation (28).

The only difference between Fig. 2b and c is the effective drug concentration D . The total fitness of the HIV-1 wild-type in Fig. 2b is $f_{\text{wt}} = 1/(1 + 100) \approx 0.01$ (see equation 4) and that in Fig. 2c is $f_{\text{wt}} = 1/(1 + 1) = 0.5$. Apparently there exists a critical total fitness below which the virus cannot survive. This is studied more rigorously in Fig. 3, where we plot the stable equilibrium HIV-1 RNA load (Fig. 3a) and the CD4⁺ T-cell count (Fig. 3b) as a function of the total fitness f_{wt} . The critical total fitness corresponds to the point where the equilibrium HIV-1 RNA drops to zero and the CD4⁺ T cell counts reaches the flat noninfected equilibrium. The critical total fitness depends on the T-cell activation rate α but has an order of magnitude of 20% of the maximum fitness. Interestingly, the equilibrium viral load is almost a step function of the total fitness (Fig. 3a). Thus, decreasing the total fitness, e.g., by giving an RT inhibitor, while maintaining it above the critical value hardly affects the equilibrium HIV-1 RNA load. Instead, the effect of changing the total fitness is largely reflected in the equilibrium CD4⁺ T-cell count.

Figure 2b in the report of Ho *et al.* (17) depicts that the per-capita growth rate of CD4⁺ T cells decreases with increasing CD4⁺ baseline counts. As shown in Fig. 2a and b, our model matches these data. The per-capita CD4⁺ T-cell growth rate in our model has a similar inverse relationship with the baseline CD4⁺ count due to two separate mechanisms. First, the growth rate decreases with the CD4⁺ counts because of our density-dependent proliferation term. Second, in our model, low CD4⁺ counts correspond to a late latency stage with higher T-cell activation rates.

Lamivudine. In a recent study, 20 patients were treated with the RT inhibitor lamivudine (35). In this study, CD4⁺ T-cell counts, serum HIV-1 RNA loads, and the frequency of three drug-resistant mutants were assessed at baseline and at 2 days and 1, 2, 3, 4, 6, and 8 weeks after the onset of treatment. Resistance to lamivudine is caused by a mutation in codon 184 of the HIV-1 RT gene, which replaces the wild-type methio-

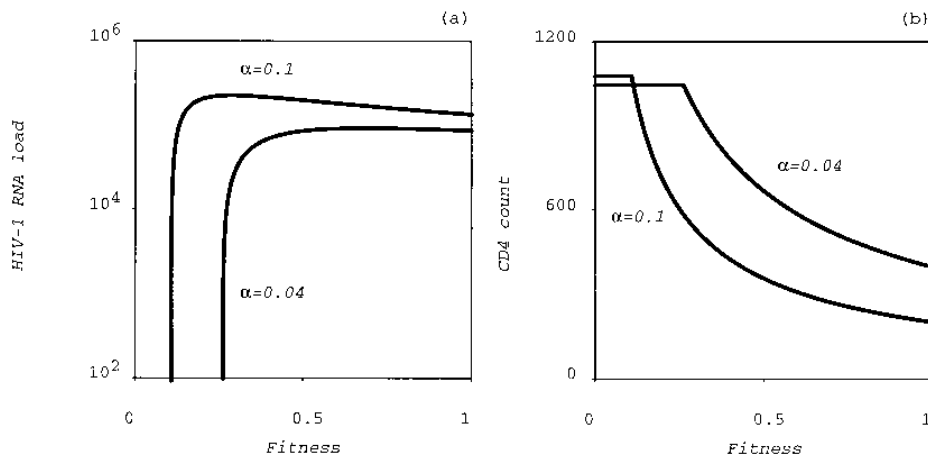


FIG. 3. The equilibrium level of the HIV-1 RNA load (a) and the CD4⁺ T-cell count (b) as a function of the total fitness (i.e., f_j) in the absence of mutation. This plot was generated by switching off mutation and by calculating the equilibrium of the wild-type virus and the total CD4⁺ count for all total fitness values between 0 and 1. Knowing the total fitness of any strain, in either the presence or the absence of the drug, one can determine from these curves the equilibrium that would be attained by that strain. The region where the equilibrium HIV-1 level becomes zero, i.e., around a total fitness $f_j \approx 0.2$, gives the critical total fitness required for eradication of that strain. Parameters are as in Fig. 2.

nine residue (ATG) with either an isoleucine (ATA) or a valine (i.e., GTG or GTA) (4, 21, 22). These mutants have a 500- to 1,000-fold reduction in susceptibility, while the drug resistance of the valine mutant seems to be somewhat higher than that of the isoleucine mutant (35). We therefore set $R_{wt} = 1$, $R_{iso} = 500$, and $R_{val} = 750$. For the fitness in the absence of the drug, we conservatively set $e_{wt} = 1$ and $e_{iso} = e_{val} = 0.99$.

Using the mutation frequencies estimated above, we obtain the mutation matrix

$$M = \begin{pmatrix} \mu_0 & \mu_2 & \mu_1 & \mu_1\mu_2 \\ \mu_1 & \mu_0 & \mu_1^2 & \mu_1 \\ \mu_2 & \mu_2^2 & \mu_0 & \mu_2 \\ \mu_1\mu_2 & \mu_2 & \mu_1 & \mu_0 \end{pmatrix}$$

where the rows and columns are ordered from the wild-type virus to the isoleucine mutant to the valine GTG mutant to the valine GTA mutant. Each row gives the mutation frequencies with which that strain is created by each of the other strains. For example, the isoleucine mutant is expected to be created from the wild-type virus most often because the second entry in the first column (i.e., μ_1) is larger than all others (ignoring the nonmutational diagonal elements). Similarly, the valine mutant is expected to mutate backward into the wild-type virus most often because the third entry in row one (i.e., μ_1) is larger than all others.

Most patients had a 1- to 3-log decrease in the HIV-1 RNA level in about a week. We therefore opt for a highly effective drug concentration; i.e., we set $D = 100$. The HIV-1 RNA and CD4⁺ cell count data differ strongly from patient to patient. Plotting the median mutant frequencies reveals that the isoleucine mutant comes first and that it is rapidly replaced by the GTG valine mutant (35). Since taking median values tends to smooth the data, one would have to compare the model behavior to that of each individual patient. Here we make a compromise by picking one patient whose HIV-1 RNA data resemble those of the median and whose CD4⁺ counts increase in response to the therapy. Thus, we pick patient C0021, who has an initial CD4⁺ count of 220 cells per μl and an HIV-1 RNA level of approximately 4×10^4 RNA copies, which is representative for the 20 patients in the study (35). We therefore set $\alpha = 0.1$, yielding $T_{tot} \approx 200$ with approximately 10%

productively infected cells. The data and the model results are depicted in Fig. 4.

The CD4⁺ cell count of patient C0021 increases marginally only, i.e., from 220 at day 0 to 280 at day 28 (Fig. 4a). Pooling the data of all 20 patients, Schuurman et al. (35) indeed report a median increase of the CD4⁺ counts of about 15% at 3 weeks. This is very low compared to the data for protease inhibitors and/or other RT inhibitors (17, 36). In our model (Fig. 4a), we find a twofold increase in the CD4⁺ counts in about 2 weeks, which deviates from our own data (35) but is in agreement with other data on protease (17, 36) and RT (8, 36) inhibitors.

In the model, the total viral RNA load reaches its minimum around day 8, peaks again around day 20, and then approaches a new equilibrium (Fig. 4b). The initial phase during which the virus load descends corresponds closely to the data (i.e., patient C0021 and the median counts (35)). In the model, the HIV-1 RNA rebound during week 2 is faster than that in the data. One has to bear in mind that our model remains an oversimplification and that a precise fit is not to be expected. A possible explanation is the absence of long-lived infected cells from our model (see Discussion).

Figure 4c depicts the fractions of the wild-type, isoleucine, and valine genotypes. The model matches the data in that both generate exactly the same evolutionary sequence. The isoleucine and valine mutants appear within 2 weeks. The valine mutant subsequently outcompetes the isoleucine mutant over a time period of a few months. For this particular patient, one could argue that the isoleucine mutant appears and disappears faster than it does in the model. There is, however, too much variation between the patients to blame this on the model. For instance, patient C0021 might have had a higher than expected initial frequency of the isoleucine mutant (see below). In both the model and the data, the fraction of GTA valine mutants always remains small (not shown). Thus, we conclude that taking the current drug resistance and mutation estimates, we can account for the correct evolutionary sequence.

Zidovudine. In another recent study, 24 asymptomatic HIV-1-infected persons were treated with zidovudine (8). Their average CD4⁺ count was 380 cells per μl . The serum HIV-1 RNA load was measured at 0, 1, 3, 6, and 9 months and at

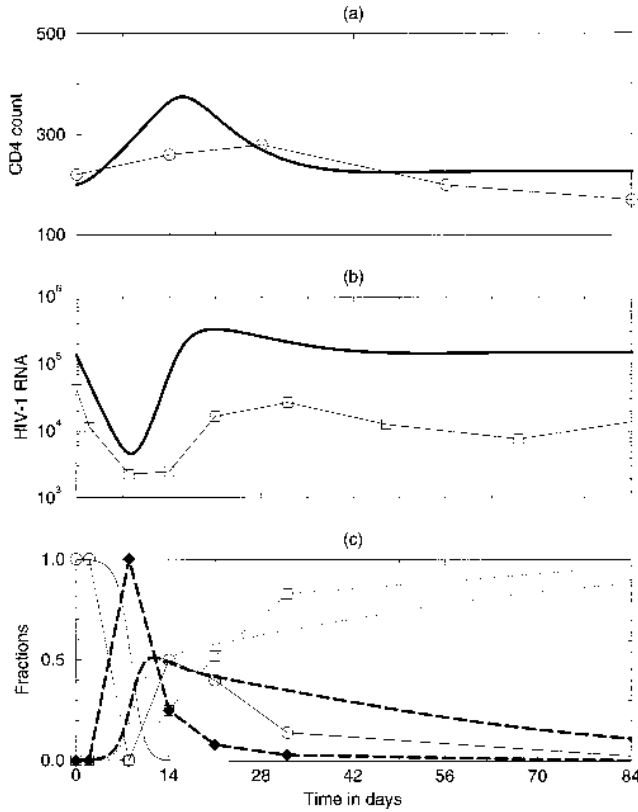


FIG. 4. CD4⁺ and HIV-1 RNA levels of a representative patient (i.e., C0021) treated with lamivudine and of the model with an effective drug concentration $D = 100$. The patient data are denoted by symbols connected by straight lines; the model behavior is denoted by the continuous lines. Setting $\alpha = 0.1$ per day, we obtain a CD4⁺ count in the infected state of $T_{\text{tot}} \approx 200$. Parameters are as in Fig. 2, but $\mu_1 = 10^{-5}$, $\mu_2 = 5 \times 10^{-6}$, for the mutant RT fitnesses we conservatively estimate $e_{\text{iso}} = e_{\text{val}} = 0.99$, and the drug resistances are estimated to be $R_{\text{iso}} = 500$ and $R_{\text{val}} = 750$. (a) CD4⁺ counts; (b) total HIV-1 RNA, (c) RNA fractions of the wild-type virus (circles), of the isoleucine mutant (diamonds), and of the valine mutant (squares).

approximately 1 and 2 years after treatment. Relative amounts of HIV-1 RNA containing mutations in RT at positions 41, 70, and 215 were assessed as described previously (8). The mutations involved in zidovudine resistance are ATG \rightarrow CTG for codon 41, AAA \rightarrow AGA for codon 70, and ACC \rightarrow TAC for codon 215. Since the mutations involve different codons, they can appear in any combination. We thus have seven strains: the wild-type V_{wt} , the mutants at positions 41 (i.e., V_{41}), 70 (i.e., V_{70}), 215 (i.e., V_{215}), and the mutants at combinations of 41 with 70 (i.e., V_{4170}), 41 with 215 (i.e., V_{41215}), and 70 with 215 (i.e., V_{70215}). The drug resistances (IC_{50} s) of the seven strains have been estimated: $R_{\text{wt}} = 1$, $R_{41} = 4$, $R_{70} = 8$, $R_{215} = 16$, $R_{4170} = 9$, $R_{41215} = 60$, and $R_{70215} = 6$ (19, 23).

Using the mutation rates estimated above, we obtain the mutation matrix

$$M = \begin{pmatrix} \mu_0 & \mu_3 & \mu_1 & \mu_3^2 & \mu_1\mu_3 & 0 & 0 \\ \mu_3 & \mu_0 & \mu_1\mu_3 & 0 & \mu_1 & \mu_3^2 & 0 \\ \mu_2 & \mu_2\mu_3 & \mu_0 & 0 & \mu_3 & 0 & \mu_3^2 \\ \mu_3^2 & 0 & 0 & \mu_0 & 0 & \mu_3 & \mu_1 \\ \mu_2\mu_3 & \mu_2 & \mu_3 & 0 & \mu_0 & 0 & 0 \\ 0 & \mu_3^2 & 0 & \mu_3 & 0 & \mu_0 & \mu_1\mu_3 \\ 0 & 0 & \mu_3^2 & \mu_2 & 0 & \mu_2\mu_3 & \mu_0 \end{pmatrix}$$

where the rows and columns are ordered as follows: wild type,

41, 70, 215, 4170, 41215, and 70215. Again, each row gives the mutation frequencies by which the strain of that row is created by each of the other strains.

The typical sequence of the three mutations as they appear in the data is 70 \rightarrow 215 \rightarrow 41 (8). Empirically, it is not known in what specific strains these mutations arise; we know only what fraction each mutation comprises of the total population. In our model, the same fractions are defined as $p_{41} = (V_{41} + V_{4170} + V_{41215})/\Sigma V_j$, $p_{70} = (V_{41} + V_{4170} + V_{41215})/\Sigma V_j$, and $p_{215} = (V_{215} + V_{41215} + V_{70215})/\Sigma V_j$. Using the parameters on the drug resistance and the mutation frequencies, we typically find the same sequence in the model, i.e., $p_{70} \rightarrow p_{215} \rightarrow p_{41}$. In the model, we can easily check in what specific strains these mutations appear. Thus, we complement the empirical data with suggestions on the precise evolutionary order.

The time scale at which the mutations appear largely depends on the effective drug concentration D . Ideally, it would be preferred to estimate D from the initial slope with which the virus RNA load declines (see Appendix). Unfortunately, this is not possible because our first data point at 1 month has missed the first minimum (which is probably at 2 weeks [24]). We therefore fit the effective drug concentration such that the time scale on which the mutants arrive is approximately correct. This gives $D = 0.5$, which means that the total fitness of the wild-type virus becomes $f_{\text{wt}} = 1/(1 + D) = 0.67$. Because such a fitness is well above the critical fitness of Fig. 3, we expect the wild-type virus to rebound.

We again compare the model behavior with the data by picking one representative patient, i.e., patient 276, whose behavior corresponds reasonably well to the median results (8). This patient has a CD4⁺ count of about 500 T cells per μl ; we therefore set $\alpha = 0.03$, yielding $T_{\text{tot}} \approx 500$. Simulating the model with our conservative fitness estimate of $e_j = 0.99$ for all drug-resistant mutants j , we again find the correct evolutionary order of the drug-resistant mutants. The 70 mutant, however, arrives far too early, and the 215 mutants tend to arrive too late. We therefore adjust the (unknown) fitness parameters such that $e_{41} = e_{70} = e_{4170} = 0.95$. The other fitnesses all involve the 215 mutation and are kept at their default value of 99%; i.e., we keep $e_{215} = e_{41215} = e_{70215} = 0.99$. This indeed slows down the 70 mutants and speeds up the 215 mutants. The sensitivity of the model behavior for these fitness parameters pinpoints the significance of determining them experimentally (work in progress; see Discussion).

Pooling the data from all cases and plotting median results, we have demonstrated a significant increase of the CD4⁺ cell count in the first few months (8). The CD4⁺ data from individual patients are very noisy, however (e.g., patient 276 in Fig. 5a). In the model, the CD4⁺ count peaks at day 60, having increased by about 30% (Fig. 5a). For an initial CD4⁺ count of 500 cells per μl , this CD4⁺ increase is in agreement with the data (17).

Comparing the HIV-1 RNA levels of the model and the data is difficult because we have missed the true minimum in our data. The model shows a minimum RNA level at about 3 weeks after the onset of treatment, which is in agreement with other recent data (24). Nevertheless, the model behavior is a little too fast because the total virus RNA rebounds such that we have a peak at 2 to 3 months. In the data, the HIV-1 RNA recovery takes longer (Fig. 5b and reference 8). The observation that the model is somewhat too fast is the same (minor) discrepancy between model and data that we have discussed above for the lamivudine data.

The evolutionary sequence in the model and the data are again in close correspondence (Fig. 5c). The first drug-resistant mutant is the codon 70 amino acid change. This mutant is

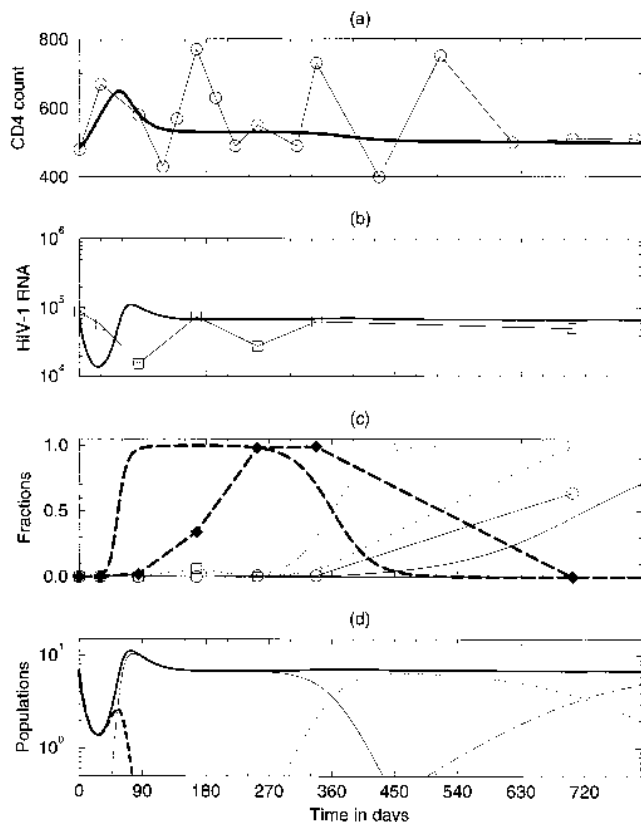


FIG. 5. The evolution of drug-resistant mutants to zidovudine for a representative patient (i.e., 276) and for the model with $D = 0.5$. The patient data are denoted by symbols connected by straight lines; the model behavior is denoted by the continuous lines. Setting $\alpha = 0.03$ per day, we obtain a $CD4^+$ count in the infected state of $T_{tot} = 500$. Assuming a higher efficacy for the 215 mutant, we set the fitness of the six mutant strains to $e_{41} = e_{70} = e_{4170} = 0.95$ and $e_{215} = e_{41215} = e_{70215} = 0.99$. The resistance parameters were previously estimated as $R_{41} = 4$, $R_{70} = 8$, $R_{215} = 16$, $R_{4170} = 9$, $R_{41215} = 60$, and $R_{70215} = 6$ (19, 23). Other parameters are as in Fig. 4, with the addition of $\mu_3 = 10^{-6}$. (a) $CD4^+$ T-cell counts; (b) total HIV-1 RNA; (c) RNA fractions of the 41 mutant (circles), of the 70 mutant (diamonds), and of the 215 mutant (squares). (d) HIV-1 genotypes at arbitrary concentrations. Heavy solid line, total HIV-1 RNA; heavy dashed line, wild-type RNA; light solid line, the 70 mutant; dotted line, the 215 mutant; the dash-dotted line, the 41215 mutant.

slowly replaced by the 215 mutation. The latter strain subsequently also acquires the codon 41 mutation. The 70 mutation confers relatively little resistance (i.e., $R_{70} = 8$) but is generated at highest frequency by RT mutations in the wild-type virus. Thus, we again conclude that the current empirical estimates for the drug resistances and mutation frequencies of the HIV-1 variants are sufficient for explaining the evolutionary order observed in the clinical data. The evolutionary rates in the model are again somewhat too fast.

The clinical data on the fractions of the mutations are complemented with the absolute genotype densities, as suggested by the model, in Fig. 5d. In the model, the wild-type population initially decreases but rebounds after about 3 weeks. Thus, the initial increase of the viral load after 1 month is largely due to a rebound of the wild-type virus. We have reported similar behavior in our clinical data (8). In the model, the wild-type virus increases due to the increased availability of target $CD4^+$ T cells, which compensates for the antiviral effect of the zidovudine treatment (see also Fig. 3). Around day 60, the wild-type virus starts to decline again due to competition with the 70 mutant, which in the presence of the drug (i.e., for $D =$

0.5) has a higher fitness than the wild-type virus. Similar model behavior has also been reported before (14, 28).

The competition between the wild-type virus and the 70 mutant slows down the development of drug resistance. If we were to artificially prevent the rebound of the wild-type virus, the $CD4^+$ target cell levels would increase even further, allowing the 70 mutant to develop faster. This was tested in the model by artificially decreasing the wild-type density during its rebound phase (not shown). We conclude that ecological competition processes determine the evolutionary time course of resistance development. Figure 5d shows that the 215 mutant is slowly replaced by the 41215 strain, which combines the codon 41 and 215 mutations. Thus, the late rise in the 41 fraction in Fig. 5c is due to the outgrowth of the 41215 combination.

Variation. Although most patients adhere to the typical picture depicted in Fig. 5, there is wide variation between the patients (8). The stochasticity of the mutation process is a very likely source of the variation. In the present model, we have no stochasticity: mutation is implemented as a continuous process. Elsewhere we have illustrated the effect of stochasticity in the evolutionary time course by altering the initial densities of the mutants (8).

DISCUSSION

A host-parasite model is an important tool for understanding the complex evolutionary process of the development of drug resistance. The model qualitatively accounts for the evolutionary sequence of drug-resistant mutants in two clinical data sets with different RT-inhibiting drugs (8, 35), has the correct time scales for the changes in the HIV-1 RNA load and the $CD4^+$ cell counts (17, 36), and has approximately correct time scales for the appearance of the drug-resistant mutants (8, 35). The results show that (i) the observed time scale differences between lamivudine and zidovudine can be explained by a difference in the efficacies of the two drugs, (ii) the precise evolutionary order of the drug-resistant mutants can be fully explained by a combination of the current estimates for the mutation frequencies and for the drug resistances of the mutants, and (iii) the observed rebound of the wild-type HIV-1 RNA load in the zidovudine data can be explained by the lower efficacy of zidovudine. In the model, there is a critical treatment level below which the wild-type HIV-1 RNA load can rebound before the appearance of the first drug-resistant mutant. Finally, the model complements our understanding of the zidovudine data by suggesting which genotypes are responsible for the codon fractions that we measure.

There are also important differences between the model behavior and the clinical data, however. First, the increase in the $CD4^+$ T-cell counts during the first weeks of treatment is too large in the model. The T-cell growth rate in our model is determined by the T-cell activation rate α . Thus, one could argue that a simple solution for this discrepancy would be to select a lower T-cell activation rate. This issue seems to be more complicated, however. Recent clinical data show that in patients treated with highly effective combinations of antiretroviral drugs, the $CD4^+$ T-cell counts fail to fully recover. Thus, it seems that at undetectably low viral loads, the $CD4^+$ compartment remains affected. For instance, the destruction of lymphoid tissue by the HIV infection could decrease the equilibrium $CD4^+$ cell count (13), i.e., could decrease the T_{max} parameter of our model (7). Such an effect would put a realistic limit to the recovery of the $CD4^+$ levels in our model. Second, a large-scale clinical study on the effects of lamivudine and zidovudine (10) reports a sustained 0.5- to 1-log decrease

in the viral load after a year of treatment. This is a surprising finding because by the evolution of drug resistance, one expects hardly any effects of these drugs after a year of treatment. The only explanation seems that the drug-resistant mutants have a much lower fitness than we have assumed. We have seen in Fig. 3, however, that in our model, the equilibrium viral load is almost a step function of the total fitness. Thus, in our model, a 0.5- to 1-log change in the equilibrium viral load cannot be realistically attributed to a change in the total fitness.

With respect to the parameter values, the fitness values e_j in the absence of the drug remain the most important unknowns. Recent *in vivo* estimates for zidovudine-resistant mutants suggest that in the absence of zidovudine, the fitness differences between mutants may be considerable, i.e., 10 to 40% (16). For lamivudine, only preliminary *in vitro* estimates are available. Estimating these fitness values *in vitro* is extremely difficult because the estimates depend strongly on the type of target cell used in the assay (1). In some of the cell lines, however, it also seems that in the absence of lamivudine, the fitness of the valine mutant in the lamivudine study is considerably higher than that of the isoleucine mutant (1, 30a). Thus, our conservative estimate of making the fitness of all mutants 99% of that of the wild type need not be realistic. However, in our model, the total fitness is the product of drug resistance and the fitness of the absence of the drug (equation 4). Thus, if the fitness of the valine mutant were indeed higher than that of the isoleucine mutant in the lamivudine study (1, 30a), i.e., if $e_{\text{val}} > e_{\text{iso}}$, we would obtain similar results in our model when we give the two mutants similar drug resistances, i.e., set $R_{\text{val}} \approx R_{\text{iso}}$.

An obvious extension of our model would be to allow for a small subpopulation of long-lived productively infected cells. This could significantly alter the evolutionary dynamics because early strains will linger much longer. This could explain why in our model the drug-resistant mutants appear a little too fast and the wild-type virus disappears too early. The distinction between quiescent and activated CD4⁺ T cells in our model is not required for explaining our data. This feature of our model, however, allows us to model disease progression by an increase in the general T-cell activation rate, which is in agreement with current ideas (12) and which yields the realistic progression scheme of a slowly increasing HIV-1 RNA load with concomitant slow decrease of the CD4⁺ T-cell count (7). This behavior is otherwise difficult to obtain with host-parasite models.

In our model, we have ignored variations in the antiviral immune response by keeping the turnover of productively infected cells constant. As a consequence, the HIV infection in our model is target cell limited (6, 7). The same is true for the previous models for the evolution of drug resistance to RT inhibitors (14, 28). One can, however, account for the same clinical data with immune-control models in which the level of the immune response changes rapidly to the changes in the viral load that are induced by the antiretrovirus treatments (7).

In summary, with our mathematical model, we have been able to increase our understanding of the evolutionary dynamics of HIV-1 drug resistance. Armed with these insights, one can test our assumptions, study alternative models, and try to fill in the unknown parameters.

APPENDIX

Right after the administration of the RT inhibitors, the viral RNA load drops. In the data (8, 35) and in the model, this decline is approximately linear on a log scale. The slope of this decline can be used to estimate the effective drug concentration D . The maximum slope is determined by the turnover rate δ_I of productively infected cells. This turnover rate was previously estimated by assuming that the

drug is 100% effective (17, 36). This assumption of an almost 100% effective drug concentration is probably reasonable for the protease inhibitors (17, 36) and for lamivudine (35) but is definitely incorrect for zidovudine (8). Thus, we here estimate the relationship between the predicted slope θ and the effective drug concentration D .

Since the level of drug-resistant mutants is low at the onset of treatment, we ignore them and consider the wild-type virus only. This simplifies equation 3 to

$$\frac{dI_{\text{wt}}}{dt} = I_{\text{wt}} \left(\frac{\beta\mu_0 T}{1+D} - \delta_I \right) \quad (\text{A1})$$

where we have substituted $V_{\text{wt}} = I_{\text{wt}}$. This nonlinear equation can be solved for the time period during which virus declines when we make the approximation that the target cell level T remains constant or changes only slowly. Given this approximation, the slope is

$$\theta = \frac{\beta\mu_0 T(0)}{1+D} - \delta_I \quad (\text{A2})$$

where $T(0)$ is the number of activated cells at day 0. We can easily check that if the drug is 100% effective, i.e., if $D \rightarrow \infty$, the slope is given by the turnover rate of productively infected cells, i.e., $\theta = -\delta_I$ (17, 36).

We have modeled the lamivudine data and the protease inhibitor data by setting the effective drug concentration to an arbitrary large value, i.e., $D = 100$. The effective drug concentration can be evaluated in terms of the fitness of the wild-type virus, i.e., by $1/(1+D)$, which for $D = 100$ is approximately zero. Hence $D = 100$ is approximately 100% effective. We can check the predicted slope for a CD4⁺ count of approximately 200 cells [i.e., for a target cell level $T(0) = 11$] by evaluating equation A2,

$$\theta = \frac{0.05 \times 0.95 \times 11}{1+100} - 0.5 \approx 5 \times 10^{-3} - 0.5 \approx -0.5 \quad (\text{A3})$$

which also shows that for $D = 100$, the slope is approximately $-\delta_I$, irrespective of the number of activated CD4⁺ cells in the range of interest.

Although the slopes with which the virus RNA levels decline in the zidovudine data cannot be estimated because our first data point at 1 month is 2 weeks later than the true minimum (24), it is clear that patients treated with zidovudine typically have much smaller slopes. Zidovudine is less effective than lamivudine or ritonavir. Thus, in terms of the total fitness of the wild-type virus, we can no longer approximate $1/(1+D) \approx 0$, which means that we precisely have to know the effective drug concentration. In fact, if earlier samples of the RNA load were available, one could use equation A2 to estimate the effective drug concentration D from the initial slope at which viral RNA declines if all other parameters are known.

ACKNOWLEDGMENTS

This work was performed during a visit of N. I. Stilianakis to Utrecht University and a visit of R. J. De Boer to the Santa Fe Institute. N. I. Stilianakis thanks the Netherlands Science Foundation for supporting his visit to the Theoretical Biology group in Utrecht. R. J. De Boer thanks Alan S. Perelson and the Santa Fe Institute for their Theoretical Immunology Program supported by the Joseph P. and Jeanne M. Sullivan Foundation. N. I. Stilianakis now is a postdoctoral fellow at the Los Alamos National Laboratory supported by the German Cancer Research Centre.

REFERENCES

- Back, N. K. T., M. Nijhuis, W. Keulen, C. A. B. Boucher, B. B. Oude Essink, A. B. P. Van Kuilenburg, A. H. Van Gennips, and B. Berkhout. 1996. Reduced replication of 3TC-resistant HIV-1 variants in primary cells due to a processivity defect of the reverse transcriptase enzyme. *EMBO J.* **15**:4040-4049.
- Bofill, M., A. Mocroft, M. Lipman, E. Medina, N. J. Borthwick, C. A. Sabin, A. Timms, M. Winter, L. Baptista, M. A. Johnson, C. A. Lee, A. N. Phillips, and G. Janossy. 1996. Increased numbers of primed CD8⁺, CD38⁺, CD5RO⁺ T cells predict the decline of CD4⁺ T cells in HIV-1-infected patients. *AIDS* **10**:827-834.
- Boucher, C. A. B., M. Tersmette, J. M. A. Lange, P. Kellam, R. E. Y. De Goede, B. J. W. Mulder, G. Darby, J. Goudsmit, and B. A. Larder. 1990. Zidovudine sensitivity of human immunodeficiency viruses from high-risk, symptom-free individuals during therapy. *Lancet* **336**:585-590.
- Boucher, C. A. B., E. O'Sullivan, B. J. W. Mulder, C. Ramautarsing, P. Kellam, G. Darby, J. M. A. Lange, J. Goudsmit, and B. A. Larder. 1992. Ordered appearance of zidovudine resistance mutations during treatment of 18 human immunodeficiency virus-positive subjects. *J. Infect. Dis.* **165**:105-110.
- Coffin, J. M. 1995. HIV-1 population dynamics *in vivo*: implications for

- genetic variation, pathogenesis, and therapy. *Science* **267**:483–489.
6. **De Boer, R. J., and C. A. B. Boucher.** 1996. Anti-CD4 therapy for AIDS suggested by mathematical models. *Proc. R. Soc. Lond. B* **263**:899–905.
 7. **De Boer, R. J., and A. S. Perelson.** Target cell limited and immune control models of HIV infection: a comparison. Submitted for publication.
 8. **De Jong, M. D., J. Veenstra, N. I. Stilianakis, R. Schuurman, J. M. A. Lange, R. J. De Boer, and C. A. B. Boucher.** 1996. Host-parasite dynamics and outgrowth of virus containing a single K70R amino acid change in reverse transcriptase are responsible for the loss of HIV-1 RNA load suppression by zidovudine. *Proc. Natl. Acad. Sci. USA* **93**:5501–5506.
 9. **Embretson, J., M. Zupancic, J. L. Ribas, A. Burke, P. Racz, K. Tenner-Racz, and A. T. Haase.** 1993. Massive covert infection of helper T lymphocytes and macrophages by HIV-1 during the incubation period of AIDS. *Nature* **362**:359–362.
 10. **Eron, J. J., S. L. Benoit, J. Jemsek, R. D. MacArthur, J. Santana, J. Quinn, D. R. Kuritzkes, M. A. Fallon, and M. Rubin.** 1995. Treatment with lamivudine, zidovudine, or both in HIV-positive patients with 200 to 500 CD4⁺ cells per cubic millimeter. *N. Engl. J. Med.* **333**:1662–1669.
 11. **Essunger, P., and A. S. Perelson.** 1994. Modelling HIV-1 infection of CD4⁺ T-cell subpopulations. *J. Theor. Biol.* **170**:367–391.
 12. **Fauci, A. S.** 1993. Multifactorial nature of human immunodeficiency virus diseases: implications for therapy. *Science* **262**:1011–1018.
 13. **Feinberg, M. B.** 1996. Changing the natural history of HIV disease. *Lancet* **348**:239–246.
 14. **Frost, S. D. W., and A. R. McLean.** 1994. Quasispecies dynamics and the emergence of drug resistance during zidovudine therapy of HIV-1 infection. *AIDS* **8**:323–332.
 15. **Goudsmit, J., A. De Ronde, D. D. Ho, and A. S. Perelson.** 1996. HIV-1 fitness in vivo: Calculations based on a single zidovudine resistance mutation at codon 215 of reverse transcriptase. *J. Virol.* **70**:5662–5664.
 16. **Goudsmit, J., A. De Ronde, E. R. De Rooij, and R. J. De Boer.** Broad spectrum of in vivo fitness of HIV-1 subpopulations differing at reverse transcriptase codons 41 and 215. Submitted for publication.
 17. **Ho, D. D., A. U. Neumann, A. S. Perelson, W. Chen, J. M. Leonard, and M. Markowitz.** 1995. Rapid turnover of plasma virions and CD4 lymphocytes in HIV-1 infection. *Nature* **373**:123–126.
 18. **Holford, N. H., and L. B. Sheiner.** 1982. Kinetics of pharmacologic response. *Pharmacol. Ther.* **16**:143–166.
 19. **Kellam, P., C. A. B. Boucher, and B. A. Larder.** 1992. Fifth mutation in human immunodeficiency virus type 1 reverse transcriptase contributes to the development of high-level resistance to zidovudine. *Proc. Natl. Acad. Sci. USA* **89**:1934–1938.
 20. **Keulen, W., C. A. B. Boucher, and B. Berkhout.** 1996. Nucleotide substitution patterns can predict the requirements for drug-resistance of HIV-1 proteins. *Antiviral Res.* **31**:45–57.
 21. **Larder, B. A., G. Darby, and D. D. Richman.** 1989. HIV-1 with reduced sensitivity to zidovudine (AZT) isolated during prolonged therapy. *Science* **243**:1731–1734.
 22. **Larder, B. A., and S. D. Kemp.** 1989. Multiple mutations in HIV-1 reverse transcriptase confer high-level resistance to zidovudine (AZT). *Science* **246**:1155–1158.
 23. **Larder, B. A., P. Kellam, and S. D. Kemp.** 1991. Zidovudine resistance predicted by direct detection of mutations in DNA from HIV-infected lymphocytes. *AIDS* **5**:137–144.
 24. **Loveday, C., S. Kaye, M. Tenant-Flowers, M. Semple, U. Ayliffe, I. V. D. Weller, and R. S. Tedder.** 1995. HIV-1 RNA serum-load and resistant viral genotypes during early zidovudine therapy. *Lancet* **345**:820–824.
 25. **Mackall, C. L., C. V. Bare, L. A. Granger, S. O. Sharrow, J. A. Titus, and R. E. Gress.** 1996. Thymic-independent T cell regeneration occurs via antigen-driven expansion of peripheral T cells resulting in a repertoire that is limited in diversity and prone to skewing. *J. Immunol.* **156**:4609–4616.
 26. **Malone, J. L., T. E. Simms, G. C. Gray, K. F. Wagner, J. R. Burger, and D. S. Burke.** 1990. Sources of variability in repeated T-helper lymphocyte counts from human immunodeficiency virus type 1 infected patients: total lymphocyte counts fluctuation and diurnal cycle are important. *J. Acquired Immune Defic. Syndr.* **3**:144–151.
 27. **Mansky, L. M., and H. M. Temin.** 1995. Lower in vivo mutation rate of human immunodeficiency virus type 1 than that predicted from the fidelity of purified reverse transcriptase. *J. Virol.* **69**:5087–5094.
 28. **McLean, A. R., and M. A. Nowak.** 1992. Competition between zidovudine-sensitive and zidovudine-resistant strains of HIV. *AIDS* **6**:71–79.
 29. **McLean, A. R., and C. A. Michie.** 1995. In vivo estimates of division and death rates of human lymphocytes. *Proc. Natl. Acad. Sci. USA* **92**:3707–3711.
 30. **Najera, L., A. Huguin, M. E. Quinones-Mateu, M. A. Munoz-Fernandez, R. Najera, C. Lopez-Galindez, and E. Domingo.** 1995. *pol* gene quasispecies of human immunodeficiency virus: mutations associated with drug resistance in virus from patients undergoing no drug therapy. *J. Virol.* **69**:23–31.
 - 30a. **Nijhuis, M., et al.** Unpublished data.
 31. **Pantaleo, G., C. Graziosi, J. F. Demarest, L. Butini, M. Montroni, C. H. Fox, J. M. Orenstein, D. P. Kotler, and A. S. Fauci.** 1993. HIV-1 infection is active in lymphoid tissue during the clinically latent stage of disease. *Nature* **362**:355–358.
 32. **Perelson, A. S., D. E. Kirschner, and R. J. De Boer.** 1993. Dynamics of HIV-1 infection of CD4⁺ T cells. *Math. Biosci.* **114**:81–125.
 33. **Perelson, A. S., A. U. Neumann, M. Markowitz, J. M. Leonard, and D. D. Ho.** 1996. HIV-1 dynamics in vivo: virion clearance rate, infected cell lifespan and viral generation time. *Science* **271**:1582–1586.
 34. **Richman, D. D., J. M. Grimes, and S. W. Lagakos.** 1990. Effect of stage of disease and drug dose on zidovudine susceptibilities of isolates of human immunodeficiency virus. *J. Acquired Immune Defic. Syndr.* **3**:743–746.
 35. **Schuurman, R., M. Nijhuis, R. Van Leeuwen, P. Schipper, D. De Jong, P. Collis, S. A. Danner, J. Mulder, C. Loveday, C. Christopherson, S. Kwok, J. Sninsky, and C. A. B. Boucher.** 1995. Rapid changes in human immunodeficiency virus type 1 RNA load and appearance of drug-resistant virus populations in persons treated with lamivudine. *J. Infect. Dis.* **171**:1411–1419.
 36. **Wei, X., S. K. Ghosh, M. E. Taylor, V. A. Johnson, E. A. Emini, P. Deutsch, J. D. Lifson, S. Bonhoeffer, M. A. Nowak, B. H. Hahn, M. S. Saag, and G. M. Shaw.** 1995. Viral dynamics in human immunodeficiency virus type 1 infection. *Nature* **373**:117–122.